Published in final edited form as:
Shock. 2012 November ; 38(5): 532–542. doi:10.1097/SHK.0b013e31826c5b19.

Radiation Combined with Thermal Injury Induces Immature Myeloid Cells

April Elizabeth Mendoza[1], **Crystal Judith Neely**[2], **Anthony G. Charles**[1], **Laurel Briane Kartchner**[1], **Willie June Brickey**[2], **Amal Lina Khoury**[1], **Gregory D. Sempowski**[3], **Jenny P.Y. Ting**[2], **Bruce A. Cairns**[1,2], and **Robert Maile**[1,2]

[1]Department of Surgery, University of North Carolina at Chapel Hill, Chapel Hill, North Carolina

[2]Department of Microbiology and Immunology, University of North Carolina at Chapel Hill, Chapel Hill, North Carolina

[3]Duke Human Vaccine Institute, Duke University Medical Center, Durham, North Carolina

Abstract

The continued development of nuclear weapons and the potential for thermonuclear injury necessitates the further understanding of the immune consequences after radiation combined with injury (RCI). We hypothesized that sub-lethal ionization radiation exposure combined with a full thickness thermal injury would result in the production of immature myeloid cells. Mice underwent either a 20% total body surface area (TBSA) full-thickness contact burn or sham procedure followed by a single whole body dose of 5-Gy radiation. Serum, spleen and peripheral lymph nodes were harvested at 3 and 14 days post-injury. Flow cytometry was performed to identify and characterize adaptive and innate cell compartments. Elevated pro- and anti-inflammatory serum cytokines and profound leukopenia were observed after RCI. A population of cells with dual expression of the cell surface markers Gr-1 and CD11b were identified in all experimental groups, but was significantly elevated after burn alone and RCI at 14 days post-injury. In contrast to the T-cell suppressive nature of myeloid-derived suppressor cells (MDSC) found after trauma and sepsis, myeloid cells after RCI augmented T-cell proliferation and were associated with a weak but significant increase in IFN-γ and a decrease in IL-10. This is consistent with previous work in burn injury indicating that a MDSC-like population increases innate immunity. RCI results in the increase of distinct populations of $Gr\text{-}1^+$ $CD11b^+$cells within the secondary lymphoid organs, and we propose these immature inflammatory myeloid cells provide innate immunity to the severely injured and immunocompromised host.

Keywords

radiation; thermal; injury; myeloid-derived suppressor cells; inflammatory monocytes

Introduction

The recent Tohoku tsunami and resulting Fukushima Dai-ichi nuclear accident have revealed the limited therapeutic countermeasures available after a radiological catastrophe. The increasing sophistication of terrorist threats and the continued development of enriched

Correspondence & requests for reprints to: April E. Mendoza, MD, University of North Carolina School of Medicine, Department of Surgery, 605 Mary Ellen Jones, Campus Box 7290, Chapel Hill, NC 27599, Fax: 919-966-8416, Phone: (504) 975-4300, amendo@lsuhsc.edu.

There are no conflicts of interest to disclose.

nuclear energy sources by politically unstable regimes have renewed the interest in the health outcomes after radiation exposure with or without a combined injury. The most significant nuclear events are epitomized by the Hiroshima and Nagasaki nuclear detonation and the Chernobyl nuclear accident which resulted in the majority of casualties with radiation exposure complicated by thermal injury (1–3). There have since been 426 reported major radiation accidents worldwide (3). Radiation combined injury (RCI) is defined as any injury coupled with radiation exposure (2). The National Institutes of Allergy and Infectious Disease have identified RCI as an important topic for national security requiring further scientific investigation (2). RCI is associated with decreased survival after non-lethal radiation exposures in many animal models as the result of myelodepression, sepsis and multi-organ failure (4).

Current medical management of RCI involves supportive therapy with an emphasis on addressing the consequences of immunosuppression. Treatment involves fluid resuscitation, prophylactic antibiotics, administration of specific blood products or hematopoietic stem cells, and recombinant cytokine therapy (3). Our group and others have previously shown that severe burn injury results in the development of a dysfunctional immune response similar to RCI resulting in sepsis, multi-organ failure and death (5–8). The proliferation of Gr-1$^+$ CD11b$^+$cells has been described after burn injury, trauma and sepsis (9–12). This phenomenon is believed to occur as a result of emergency myelopoiesis, which increases the production of terminally undifferentiated cell types (9). Gr-1, which includes Ly6C and Ly6G, and CD11b are cell surface markers often observed on myeloid cells including MDSC, inflammatory monocytes and polymorphonuclear cells (PMN) (10–14). Classically MDSC are defined by their myeloid origin and their ability to suppress T-cell proliferation (14, 15). The suppressive function of MDSC has been demonstrated after trauma and sepsis (9, 12, 16). After trauma, Gr-1$^+$ CD11b$^+$ cells decrease CD3/CD28-mediated T-cell proliferation by an arginase-dependent mechanism and increase nitric oxide production (12, 17). However, MDSC can produce pleiotropic cytokine responses, consistent with inflammatory monocytes and similar to the M1 and M2 characteristics seen in macrophages (17). Serum from RCI animals has been shown to stimulate the growth of hematopoietic stem cell colonies by culture (18). Yet, the specific target cell type under these conditions has not been identified. We hypothesize that RCI will result in the elevation of specific pro- and anti-inflammatory serum cytokines with a corresponding lymphopenia and neutropenia. However, we propose that RCI will induce an increase in Gr-1$^+$CD11b$^+$ cells, and these cell populations will characterize the innate immune response in the severely injured host.

Materials and Methods

Experimental animals

Female C57BL/6 mice ages between 8 and 12 weeks (18–24 g weight) were purchased from Taconic Farms (Germantown, NY). All mice used in the study were maintained under specific pathogen-free conditions at the American Association of Laboratory Animal Care-accredited University of North Carolina Department of Laboratory Animal Medicine Facilities.

Combined Irradiation and Burn Injury

All protocols were in accordance with the National Institutes of Health guidelines and approved by the University of North Carolina Institutional Animal Care and Use Committee. The burn injury has been previously described (5, 6, 19). Animals either received a 0-, 2-, 5-, 6- or 9-Gy (dose rate: 1.28 Gy/min) whole-body dose of ionizing radiation by exposure to ^{137}Cesium (J.L. Shepherd & Associates, San Fernando, CA) immediately following the burn and sham procedure.

In more detail, the burn injury procedure consists of the administration of anesthesia by isoflurane vapor inhalation (Pitman-Moore, WA Crossing, NJ) followed by the removal of dorsal and flank hair by clippers. Mice received a subcutaneous injection of buprenorphine (3mg/kg body weight) for pain control immediately before burn injury. A full-thickness contact burn of 20% total body surface area (TBSA) was produced by applying a copper rod, heated in 100°C boiling water, to the animal's dorsum and flank for 10 seconds. Four applications of a 65 g rod (1.9 cm in diameter) were used to produce the wound. Mice were resuscitated with an intraperitoneal injection of Lactated Ringer's solution (0.1mL/gm body weight). Animals were returned to individual cages and provided food and morphinated water throughout the experiment. Sham controls with a 0% TBSA burn underwent all described interventions except for application of the heated copper rods. Mortality from burn injury is negligible (<1%) with this protocol. Within one hour after burn and sham procedure, mice were irradiated.

Mice were monitored twice daily for survival for up to one week and once daily thereafter. Gross appearance and behavior were closely monitored. Body weight (grams) was recorded on the day of the experiment and on days 3, 7, and 14. Mice were euthanized at 3 days, 14 days, and 21 days post-injury for analysis of serum, spleen, and peripheral lymph nodes (PLN). Blood was obtained by cardiac puncture, and underwent centrifugation for 20 minutes at 3000The serum was stored at −80°C until further processing.

Analysis of Cytokines

Cytokine analysis was performed through a 20-plex cytokine microbead array system (Invitrogen, Carlsbad, CA) at the Center for Medical Countermeasures Against Radiation (CMCR) core facility of Duke University Medical Center. The microbead array allowed for simultaneous measurement of the following inflammatory mediators in a 50μl sample of serum or supernatant: interleukin (IL)-5, IL-6, IL-10, IL-12, monocyte chemotactic protein (MCP)-1, interferon-inducible protein 10 (IP-10, CXCL-10), monokine induced by IFN-γ (MIG), macrophage inflammatory protein (MIP)-1alpha, fibroblast growth factor (FGF), vascular endothelial growth factor (VEGF), interferon (INF)-γ, IL-1α, IL-1β, IL-6, IL-2, IL-4, IL-17, keratinocyte chemoattractant (KC), tumor necrosis factor (TNF) and granulocyte-macrophage colony stimulating factor (GM-CSF). Results were analyzed using a Bioplex Workstation (Bio-Rad Laboratories, Hercules, CA). The level of sensitivity for each microbead cytokine standard curve ranged from 4 to 63pg/ml.

Cell Preparation and Flow Cytometric Analysis

Single cell suspensions were prepared from the bone marrow, spleen and peripheral lymph nodes (PLN) of female B6 mice for flow cytometric analysis. Bone marrow was obtained from bilateral femurs. Each femur was cut on both ends and flushed with 5ml of PBS. Red blood cells were depleted from spleen and bone marrow by ACK lysis buffer (0.15M NH_4Cl, 1.0mM $KHCO_3$, 0.1mM Na_2EDTA). All antibodies were produced by BD Biosciences Pharmingen, San Diego, CA except where stated. The panel of monoclonal antibodies used for analyses were anti-CD4 (L3T4) (eBioscience, San Diego, CA), anti-CD8 [alpha] (53-6.7), anti-CD11b (M1/70), anti-Gr-1 (RB6-8C5), anti-F4/80 (BM8) (eBioscience), anti-Ly6C (AL-21), anti-Ly6G (1A8), and anti-CD31 (MEC 13.3).

Four- to five-color analyses were performed using standard methods. List mode data were collected on FACS Cyan (Dako, Ft. Collins, CO) and analyzed using Summit software (Beckman Coulter, Brea, CA).

Cell Purification

T-cells were prepared from spleens of mice. $CD4^+$ and $CD8^+$ T-cells were negatively selected by the use of magnetic antibodies specific to MHC Class II^+, $CD11b^+$, and other cell types using the BD IMagnet Mouse T lymphocyte Enrichment Set according to the manufacturer's instructions (BD Biosciences, San Diego). This enrichment assay removes cells with these magnetically-bound antibodies leaving an enriched $CD4^+$ and $CD8^+$ T-cell population. This method routinely provides us with >95% pure T-cell populations.

In order to isolate $CD11b^+$ cells, the positive fraction from the above T-cell purification underwent positive selection through magnetic nanoparticles conjugated to anti-mouse CD11b monoclonal antibodies using the BD IMagnet anti-Mouse CD11b magnetic particles according to the manufacturer's instructions (BD Biosciences). CD11b-bearing leukocytes include granulocytes, macrophages, myeloid-derived cells and other cell types.

The $CD11b^+$ cell populations were resuspended in 2% fetal bovine serum in phosphate buffer saline and counted. Cells were filtered through cell strainer caps (35-μm mesh) to obtain a single cell suspension ($0.5–2.5 \times 10^7$ cells per millilter). Surface antigens were labeled by incubating with primary antibodies with Fcγ III/II receptor block (2.4G2; BD Pharmingen) for 30 minutes in the dark at 4°C, followed by 20–30 minutes with anti-CD11b and anti-Gr-1 antibodies. All washing steps were performed in 2% fetal bovine serum in phosphate buffer saline. The stained cells were analyzed and sorted on a fluorescence-activated cell sorter [Beckman-Coulter (Dako) Fort Collins, CO]. Data were analyzed and presented using Summit software (Dako). All analyses and sorts were repeated, and purity of sorted fractions was checked by FACS reanalysis. Prior to sorting, all appropriate equipment was sterilized with 70% ethanol and sterile water and was re-sterilized between each sample.

T-cell Proliferation Assay

T-cell stimulation was performed by co-stimulation of the T-cell receptor (TCR). Purified anti-CD3 (145-2C11; Southern Biotech, Birmingham, AL) was coated on a 96-round bottom plate for 2 hours at 36.7 to 37°C and cooled at 4°C until use (<6 hours). Purified T-cells from untouched B6 mice were placed into wells at a concentration of 10^6cells/ml per well. Soluble anti-CD28 (37.51; BD Pharmingen) was added simultaneously with the purified T-cells and $Gr\text{-}1^+$ $CD11b^+$cells in a 1:1 ratio from sham, burn, radiation and RCI groups. Controls included stimulated and non-stimulated T-cell wells. Cells were incubated for 24–48 hours, then 1 μCi of [methyl-^{3}H]-thymidine (6.7 Ci/mmol; PerkinElmer, Boston, MA) was added. Incorporation of [^{3}H]-thymidine was measured 18 hours later by scintillation counting with the use of a counter (LS5000; Beckman Coulter, Fullerton, CA). Supernatant (50μl) from the T-cell proliferation assay was removed prior to the addition of ^{3}H-thymidine and stored at −20°C until further processing. Cytokine analysis was performed as previously described.

Acinetobacter baumanii intratracheal inoculation and harvest

Fresh inocula were prepared for each experiment from a frozen stock of kanamycin-resistant (ATCC: BAA-1710 strain AYE; Manassas, VA). were regrown on tryptic soy agar containing kanamycin (TSA-k) (25mg/L) for 18 hours at 37°C. Bacteria were resuspended in phosphate buffered solution.

Sham, burn, radiation (5-Gy) and RCI (5-Gy) mice were anesthetized, and received an intratracheal inoculation of 1×10^7 cells/50μl using an intratracheal aerosolizer (Penn-Century, Inc., Philadelphia, PA) at day 14 post-injury. Mice were euthanized 24 hours post-infection. The lungs, spleen and liver were harvested. Liver samples were homogenized, and inoculated onto TSA-k. Whole lung samples were finely minced. Half of the lung sample

was homogenized and inoculated onto TSA-k, and the remaining portion underwent further processing for flow cytometric analysis. Spleens were prepared as single cell suspensions. The inoculated TSA plates were incubated in 5% CO_2 at 37°C for 24 hours. Colony-forming units (CFU) were quantified per plate.

Statistical Analysis

Data are presented as means ± standard error of the means. Comparisons of means were analyzed using a Student-t test or analysis of variance (ANOVA) followed by Tukey Multiple Comparisons post-test. Body weight change over time was analyzed by ANOVA. Survival analysis was determined by using a Kaplan-Meier survival curve with log-rank significance test. Statistical significance was defined as <0.05.

Results

Burn injury combined with Radiation Reduces Survival

Burn injury alone in our model typically results in <1% mortality. Radiation alone, regardless of dose, was not associated with an increase in mortality by 21 days post-injury (Figure 1A). Burn injury followed by radiation exposure (RCI) had increased mortality especially at radiation doses greater than 5-Gy. All mice exposed to 2-Gy radiation survived thermal injury, but animals that received 5- or 9-Gy and 20%TBSA burn injury resulted in mortality ranging between 20–30% by 21 days post-injury (log rank $p < 0.05$) (Figure 1B). Mice exhibited predictable mortality between experiments in the 5-Gy group with enough survivors to perform further experiments. We and others have concluded that 5-Gy radiation is the ideal experimental model for the study of RCI (20).

Higher radiation doses prolong lymphocyte recovery and result in increased Gr-1$^+$CD11b$^+$cells in RCI

The degree of lymphopenia and lymphocyte recovery after radiation and RCI is dose-dependent (1, 2, 4, 20–24). We proposed that RCI would result in lymphopenia with a corresponding increase in Gr-1$^+$CD11b$^+$ cells. We observed significant lymphopenia after 9-Gy radiation exposure at day 21 when compared to sham, 2- and 5-Gy radiation (Figure 2A). Lymphopenia was observed after RCI with radiation doses at 5- and 9-Gy (Figure 2B). During this 21-day period, we found no differences in Gr-1$^+$CD11b$^+$ cells after radiation exposure regardless of dose (Figure 3A). Conversely, there was a significant increase of Gr-1$^+$CD11b$^+$ cells when RCI included either 5- or 9-Gy. Mice that received 2-Gy and 20%TBSA thermal injury had no differences in lymphocytes or Gr-1$^+$CD11b$^+$ cells by 21 days when compared to sham or burn (Figure 3B). RCI with 5-Gy radiation resulted in the induction of Gr-1$^+$CD11b$^+$ cells with evidence of persistent lymphopenia similar to the 9-Gy dose but with improved survival. All other radiation and RCI animals subsequently referred to in this manuscript received 5-Gy radiation.

Radiation and RCI Reduce Body Weight Early after Injury

In order to determine the effects of radiation and RCI on body weight, mice were observed twice daily for the first week after injury. Body weight was measured at the day of the initial procedure and days 3, 7 and 14 after injury or sham procedure. Weight loss was highest 3 days after radiation and RCI followed by progressive weight gain returning to baseline by day 14 in surviving mice (Figure 4). This suggests that radiation exposure results in rapid weight loss, but these changes appear transient and surviving animals return to baseline weight within 2 weeks.

Specific Systemic Inflammatory Cytokines Remain Elevated after RCI

We hypothesized that RCI would result in a mixed pro- and anti-inflammatory serum cytokines. Twenty inflammatory cytokines were analyzed at day 3 and day 14. At day 3, the pro-inflammatory cytokine IL-1β was significantly elevated after RCI (mean± SEM: 33.13±8.921 pg/ml) when compared to all experimental groups. IL-6 was elevated in both burn mice (22.79 ±8.351 pg/ml) and RCI mice (29.32±9.624 pg/ml) when compared to sham (2.370±1.369 pg/ml) and radiation alone (2.529±1.699 pg/ml). IL-10 was increased (757.5±128.7 pg/ml) while IL-12 was decreased (8.305± 1.926 pg/ml) after RCI when compared to sham (290.4±114.1 pg/ml; 38.40±5.655 pg/ml respectively) (Figure 5A).

By day 14, there were no differences in serum levels of IL-1β, IL-6 or IL-10. However, serum IL-12 had increased in both the radiation and RCI mice (Figure 5B). Unique to the RCI mice, the Th2 cytokine IL-5 and chemokines IP-10 and MCP-1 were elevated at both day 3 and day 14 post-injury, and may serve as a serum biomarker of RCI. These results suggest that RCI is associated with a mixed pro- and anti-inflammatory response.

Gr-1$^+$CD11b$^+$ Cells Increase Late after RCI in the Lymphoid Organs

We hypothesized that RCI would significantly reduce lymphocytes and neutrophils, and would result in an increased production of Gr-1$^+$CD11b$^+$ cells. Gr-1$^+$CD11b$^+$ cells represent a heterogeneous group of myeloid cells which can be further defined by their Ly6G and Ly6C expression. Gr-1$^+$ CD11b$^+$ cells after RCI include Ly6C$^+$CD11b$^+$ and Ly6G$^+$Ly6C^{int}CD11b$^+$ cells (Figure 6A). Side scatter and forward scatter of light refraction differentiate the size and granularity within these cell populations (Figure 6B). We evaluated the spleen and PLN at days 3 and 14 after burn, sham, radiation and RCI. Cell types were identified by flow cytometry, At day 3 (Figure 7) and day 14 (Figure 8) post-injury, neutrophils, macrophages and lymphocytes were significantly reduced in mice after RCI and radiation. At day 3, Gr-1$^+$CD11b$^+$ total splenic cell numbers were reduced within the radiation and RCI groups (Figure 7A1), but there were no differences in the percent of these cell populations between groups (Figure 7B). In contrast, at day 14 we observed an increase in Gr-1$^+$CD11b$^+$ cell numbers in the spleen after burn injury and RCI, which was not seen in sham mice nor mice exposed to radiation alone (Figure 8A). The percentage of Gr-1$^+$ CD11b$^+$ cells was significantly higher in mice 14 days after RCI when compared to all groups including burn injury (Figure 9). These findings were also observed in the PLN (Figure 10). We, therefore, hypothesized that Gr-1$^+$CD11b$^+$ cells observed after RCI were the result of enhanced myelopoiesis. Bone marrow collected at day 14 demonstrated increased numbers of Gr-1$^+$CD11b$^+$ cells after burn and RCI (Figure 11A). Analogous to the spleen, Gr-1$^+$ CD11b$^+$ cells in the bone marrow were comprised of Ly6G+Ly6C+CD11b+ and Ly6C+Ly6G-CD11b+ populations (Figure 11B). The expression of CD31 (PECAM-1), a progenitor and blast myeloid cell marker (9, (25), was found expressed at intermediate to high intensities in Gr-1$^+$CD11b$^+$ cells from the spleen and bone marrow following RCI (Figure 12). We concluded from these data, that Gr-1$^+$ CD11b$^+$ cells from RCI mice consist of an immature, heterogeneous population of cells which are the result of augmented myelopoiesis.

Gr-1$^+$CD11b$^+$ Cells after RCI Do Not Suppress T-Cell Proliferation or Pro-Inflammatory Cytokine Production

Gr-1$^+$ CD11b$^+$ cells can represent a variety of cell types including PMN, inflammatory monocytes and MDSC. We hypothesized that immature myeloid cells such as MDSC would arise after RCI and dampen pro-inflammatory immune responses, increasing susceptibility to opportunistic infections. When Gr-1$^+$ CD11b$^+$ cells were purified from RCI mice and cultured with CD4$^+$/CD8$^+$ T-cells, T-cell proliferation was significantly augmented (Figure 13A). Furthermore, we observed an increased production of pro-inflammatory cytokines

(IFN-γ) with a corresponding decrease in the anti-inflammatory cytokine IL-10 (Figure 13B, C). These results suggest that Gr-1$^+$ CD11b$^+$ cells in RCI do not suppress T-cell proliferation When T-cells are stimulated in the presence Gr-1$^+$ CD11b$^+$ cells from RCI mice, cytokine secretion is consistent with a Th1 response.

Pulmonary infection with Acinetobacter baumanii recruit Gr-1$^+$CD11b$^+$ cells to the site of infection and is associated with an increase in Gr-1$^+$CD11b$^+$ cells in the spleen of RCI mice

Gr-1$^+$CD11b$^+$ cells constitute a substantial component of the available immune effector cells within RCI mice at day 14 after injury. Moreover, these cells demonstrate the ability to induce Th1 cytokine production. We decided to investigate if mice after RCI could tolerate a bacterial challenge with, an opportunistic organism commonly associated with severe burn injury and ICU-associated pneumonia (26, 27). We have studied pulmonary infection in the context of burn injury, and like others have found that bacterial clearance is largely neutrophil-mediated (28–30). However, mice after RCI recruited larger numbers of Gr-1$^+$CD11b$^+$ cells to the lung (Figure 14), and Gr-1$^+$CD11b$^+$ cells increased in the spleen of RCI mice after pulmonary infection (Figure 15). Pulmonary microbial clearance was unchanged among sham, burn and RCI groups (Figure 16A). Only the radiation group (5-Gy) had decreased clearance of pulmonary. There was no difference in systemic infection, as defined by CFU recovery in the liver, among the experimental groups (Figure 16B).

Discussion

Similar to burn injury, radiation exposure can result in a variety of clinical syndromes involving multiple organ systems. Several research groups, including our laboratory, have described immune dysfunction after burn that directly results from dynamic alterations in the function of both innate and adaptive immune systems resulting in increased susceptibility to bacterial infections (5–8, 31–33). In humans, hematopoiesis is remarkably altered after radiation even at low radiation doses (1-Gy) (3). Lymphocytes appear to be especially susceptible and the rate of lymphocyte depletion has been used to signal the extent of radiation exposure (1–3, 23, 24). Irreversible and reversible hematopoietic injury can be differentiated by the rate of leukocyte decline. Mortality related to hematologic failure results from infection or bleeding from neutropenia and thrombocytopenia respectively (2). Additionally, damage to the skin and gastrointestinal integrity may exacerbate infectious complications (1).

We developed a murine model illustrating that RCI results in a mixed pro- and anti-inflammatory systemic cytokine response at days 3 and 14 after injury compared to burn and radiation alone, which may be a hallmark of RCI. At day 14, a specific Gr-1$^+$ CD11b$^+$ cell population comprises the major cell type within the peripheral lymphoid immune organs. Both inflammatory monocytes and MDSC express these surface markers, but MDSC are classically described as T-cell suppressive (13, 15, 25). MDSC have been shown to exhibit pro-and anti-inflammatory phenotypes by expression of proteins consistent with classic (M1) and alternative (M2) macrophages (17). Our serum data are consistent with a mixed inflammatory response with elevations in the pro-inflammatory cytokines IL-1β, IL-6, IL-12, MCP-1 and IP-10 and the Th2 cytokines IL-5 and IL-10. In contrast to trauma models, Gr-1$^+$ CD11b$^+$ cells after RCI do not suppress the proliferation of CD3/CD28 stimulated T-cells and appear to increase pro-inflammatory cytokines (12). Similar to sepsis models, this cell population after RCI appeared heterogenous with cell surface markers consistent of monocytic (Ly6C$^+$) and granulocytic (Ly6G$^+$) myeloid subpopulations (34). This cell population, however, is distinctly different from Gr-1$^+$CD11b$^+$ cells after sepsis as these cells did not promote a shift toward a Th2 response (34). Immature inflammatory monocytes, which express CD11b and Ly6C^{high}, can be recruited from the bone marrow to sites of inflammation and, like MDSC, have the ability to differentiate into macrophages and

dendritic cells (35–37). After thermal injury, splenic myeloid progenitor cells increase with a corresponding decrease in bone marrow progenitors (10, 38). Our results suggest there is some reconstitution of the bone marrow with immature myeloid cells after RCI when compared to radiation alone, but it is also possible that splenic myelopoiesis is increased after RCI by day 14. Total Gr-1$^+$CD11b$^+$ cells in the bone marrow are similar among sham, burn and RCI, but this is not observed in the spleen where immature myeloid cells are the predominant splenic cell type observed after RCI. Gr-1$^+$CD11b$^+$ inflammatory monocytes after burn injury secrete large amounts of pro-inflammatory cytokines and appear crucial to survival after burn injury with superimposed infection (9, 10, 11). Our data suggest that a continuum may exist between inflammatory monocytes and MDSC. This would explain the divergence of Gr-1$^+$CD11b$^+$ phenotypes observed between sepsis and injury models.

As seen in acute and chronic inflammatory processes such as major burn injury and sepsis, the continued generation and exposure to pathogen (PAMPs) and damage-associated molecules (DAMPs) overwhelm the myeloid production of terminally differentiated cells such as neutrophils, macrophages and dendritic cells resulting in emergency myelopoiesis (9). In an effort to mount a protective pro-inflammatory response to infection, there is increased production of Gr-1$^+$CD11b$^+$ cells after RCI. We observe an accumulation of immature myeloid cells in the spleen and lung after pulmonary infection with (1×10^7cfu) in RCI mice. We believe Gr-1$^+$CD11b$^+$ cells represent a population of immune effector cells adapted to protect against overt pro-inflammatory cytokine secretion, but maintain the ability to stimulate adaptive immunity and produce both pro- and anti-inflammatory cytokines.

The mechanisms of inflammatory myeloid cell differentiation and trafficking are under investigation. Myeloid cells expressing chemokine (C-C motif) receptor 2 (CCR2) respond to monocyte chemoattractant proteins (MCP-1 and -3) which recruits inflammatory monocytes from the bone marrow after infectious stimuli (36, 39, 40). We predict this mechanism may explain the increase in Gr-1$^+$CD11b$^+$ cells after RCI. We propose that an earlier induction and further differentiation of these cells could augment their innate immune functions and improve outcomes after RCI. Currently, differentiation of these monocytes into effector cells has been successful through the use of chemotherapeutic agents including all--retinoic acid, OK432 and others (41–43). Future research will need to clarify mechanisms of microbial killing, and determine if Gr-1$^+$CD11b$^+$ in the context of RCI have the ability to mature and differentiate into effective innate cell types.

Further studies are needed to delineate whether the major immune cell type of late RCI, Gr-1$^+$CD11b$^+$ cells, contribute to further immunosuppression or reconstitute the innate immunity in order to protect from invading pathogens. The expansion of Gr-1$^+$CD11b$^+$ cells after RCI may represent a therapeutic target for both burn and RCI.

Acknowledgments

This study received financial support from grants awarded by the National Institutes of Health (T32GM008450-18; R0GM076250-01A2; U19-AI067798)

Special thanks to the Flow Cytometry core facility especially Joan Kalnitsky, and the many graduate students of the UNC Department of Microbiology and Immunology especially the Kawula lab and the Serody Lab.

References

1. DiCarlo, AL.; Hatchett, RJ.; Kaminski, JM.; Ledney, GD.; Pellmar, TC.; Okunieff, P.; Ramakrishnan, N. Medical countermeasures for radiation combined injury: radiation with burn, blast, trauma and/or sepsis. report of an NIAID Workshop; March 26–27, 2007; 2008. p. 712-721.

2. DiCarlo AL, Ramakrishnan N, Hatchett RJ. Radiation combined injury: overview of NIAID research. 2010; 98:863–867.
3. DiCarlo AL, Maher C, Hick JL, Hanfling D, Dainiak N, Chao N, Bader JL, Coleman CN, Weinstock DM. Radiation injury after a nuclear detonation: medical consequences and the need for scarce resources allocation. 2011; 5 (Suppl 1):S32–44.
4. Kiang JG, Jiao W, Cary LH, Mog SR, Elliott TB, Pellmar TC, Ledney GD. Wound trauma increases radiation-induced mortality by activation of iNOS pathway and elevation of cytokine concentrations and bacterial infection. 2010; 173:319–332.
5. Buchanan IB, Maile R, Frelinger JA, Fair JH, Meyer AA, Cairns BA. The effect of burn injury on CD8+ and CD4+ T cells in an irradiation model of homeostatic proliferation. 2006; 61:1062–1068.
6. Cairns BA, Maile R, Buchanan I, Pilati D, DeSerres S, Collins EJ, Frelinger JA, Meyer AA. CD8(+) T cells express a T-helper 1--like phenotype after burn injury. 2001; 130:210–216.
7. Cho K, Adamson LK, Park J, Greenhalgh DG. Burn injury-mediated alterations in cell cycle progression in lymphoid organs of mice. 2003; 19:138–143.
8. Maekawa T, Kajihara H, Okabayashi K, Otani M, Yuge O. Impairment of splenic B and T lymphocytes in the early period after severe thermal injury: immunohistochemical and electron microscopic analysis. 2002; 28:329–339.
9. Cuenca AG, Delano MJ, Kelly-Scumpia KM, Moreno C, Scumpia PO, Laface DM, Heyworth PG, Efron PA, Moldawer LL. A paradoxical role for myeloid-derived suppressor cells in sepsis and trauma. 2011; 17:281–292.
10. Noel JG, Guo X, Wells-Byrum D, Schwemberger S, Caldwell CC, Ogle CK. Effect of thermal injury on splenic myelopoiesis. 2005; 23:115–122.
11. Noel JG, Osterburg A, Wang Q, Guo X, Byrum D, Schwemberger S, Goetzman H, Caldwell CC, Ogle CK. Thermal injury elevates the inflammatory monocyte subpopulation in multiple compartments. 2007; 28:684–693.
12. Makarenkova VP, Bansal V, Matta BM, Perez LA, Ochoa JB. CD11b+/Gr-1+ myeloid suppressor cells cause T cell dysfunction after traumatic stress. 2006; 176:2085–2094.
13. Noel G, Wang Q, Schwemberger S, Hanson C, Giacalone N, Haar L, Ogle CK. Neutrophils, not monocyte/macrophages, are the major splenic source of postburn IL-10. 2011; 36:149–155.
14. Gabrilovich DI, Nagaraj S. Myeloid-derived suppressor cells as regulators of the immune system. 2009; 9:162–174.
15. Movahedi K, Guilliams M, Van den Bossche J, Van den Bergh R, Gysemans C, Beschin A, De Baetselier P, Van Ginderachter JA. Identification of discrete tumor-induced myeloid-derived suppressor cell subpopulations with distinct T cell-suppressive activity. 2008; 111:4233–4244.
16. Munera V, Popovic PJ, Bryk J, Pribis J, Caba D, Matta BM, Zenati M, Ochoa JB. Stat 6-dependent induction of myeloid derived suppressor cells after physical injury regulates nitric oxide response to endotoxin. 2010; 251:120–126.
17. Umemura N, Saio M, Suwa T, Kitoh Y, Bai J, Nonaka K, Ouyang GF, Okada M, Balazs M, Adany R, et al. Tumor-infiltrating myeloid-derived suppressor cells are pleiotropic-inflamed monocytes/macrophages that bear M1- and M2-type characteristics. 2008; 83:1136–1144.
18. Ran XZ, Su YP, Zong ZW, Guo CH, Zheng HE, Chen XH, Ai GP, Cheng TM. Effects of serum from rats with combined radiation-burn injury on the growth of hematopoietic progenitor cells. 2007; 62:193–198.
19. Hultman CS, Cairns BA, Yamamoto H, deSerres S, Frelinger JA, Meyer AA. The 1995 Moyer Award. The effect of burn injury on allograft rejection, alloantigen processing, and cytotoxic T-lymphocyte sensitization. 1995; 16:573–580.
20. Palmer JL, Deburghgraeve CR, Bird MD, Hauer-Jensen M, Kovacs EJ. Development of a combined radiation and burn injury model. 2011; 32:317–323.
21. Augustine AD, Gondre-Lewis T, McBride W, Miller L, Pellmar TC, Rockwell S. Animal models for radiation injury, protection and therapy. 2005; 164:100–109.
22. Cheng T, Chen Z, Yan Y, Ran X, Su Y, Ai G. Experimental studies on the treatment and pathological basis of combined radiation and burn injury. 2002; 115:1763–1766.
23. Ledney GD, Elliott TB. Combined injury: factors with potential to impact radiation dose assessments. 2010; 98:145–152.

24. Messerschmidt O. Combined effects of radiation and trauma. 1989; 9:197–201.
25. Angulo I, de las Heras FG, Garcia-Bustos JF, Gargallo D, Munoz-Fernandez MA, Fresno M. Nitric oxide-producing CD11b(+)Ly-6G(Gr-1)(+)CD31(ER-MP12)(+) cells in the spleen of cyclophosphamide-treated mice: implications for T-cell responses in immunosuppressed mice. 2000; 95:212–220.
26. Keen EF 3rd, Robinson BJ, Hospenthal DR, Aldous WK, Wolf SE, Chung KK, Murray CK. Prevalence of multidrug-resistant organisms recovered at a military burn center. 2010; 36:819–825.
27. Wisplinghoff H, Perbix W, Seifert H. Risk factors for nosocomial bloodstream infections due to Acinetobacter baumannii: a case-control study of adult burn patients. 1999; 28:59–66.
28. Breslow JM, Meissler JJ Jr, Hartzell RR, Spence PB, Truant A, Gaughan J, Eisenstein TK. Innate immune responses to systemic Acinetobacter baumannii infection in mice: neutrophils, but not interleukin-17, mediate host resistance. 2011; 79:3317–3327.
29. Jacobs AC, Hood I, Boyd KL, Olson PD, Morrison JM, Carson S, Sayood K, Iwen PC, Skaar EP, Dunman PM. Inactivation of phospholipase D diminishes Acinetobacter baumannii pathogenesis. 2010; 78:1952–1962.
30. Qiu H, KuoLee R, Harris G, Chen W. High susceptibility to respiratory Acinetobacter baumannii infection in A/J mice is associated with a delay in early pulmonary recruitment of neutrophils. 2009; 11:946–955.
31. Mannick JA, Rodrick ML, Lederer JA. The immunologic response to injury. 2001; 193:237–244.
32. Gough DB, Moss NM, Jordan A, Grbic JT, Rodrick ML, Mannick JA. Recombinant interleukin-2 (rIL-2) improves immune response and host resistance to septic challenge in thermally injured mice. 1988; 104:292–300.
33. Silver GM, Gamelli RL, O'Reilly M, Hebert JC. The effect of interleukin 1 alpha on survival in a murine model of burn wound sepsis. 1990; 125:922–925.
34. Delano MJ, Scumpia PO, Weinstein JS, Coco D, Nagaraj S, Kelly-Scumpia KM, O'Malley KA, Wynn JL, Antonenko S, Al-Quran SZ, et al. MyD88-dependent expansion of an immature GR-1(+)CD11b(+) population induces T cell suppression and Th2 polarization in sepsis. 2007; 204:1463–1474.
35. Rose S, Misharin A, Perlman H. A novel Ly6C/Ly6G-based strategy to analyze the mouse splenic myeloid compartment. 2012; 81:343–350.
36. Tacke F, Randolph GJ. Migratory fate and differentiation of blood monocyte subsets. 2006; 211:609–618.
37. Serbina NV, Jia T, Hohl TM, Pamer EG. Monocyte-mediated defense against microbial pathogens. 2008; 26:421–452.
38. Silva KD, Gamelli RL, Shankar R. Bone marrow stem cell and progenitor response to injury. 2001; 9:495–500.
39. Serbina NV, Pamer EG. Monocyte emigration from bone marrow during bacterial infection requires signals mediated by chemokine receptor CCR2. 2006; 7:311–317.
40. Jia T, Serbina NV, Brandl K, Zhong MX, Leiner IM, Charo IF, Pamer EG. Additive roles for MCP-1 and MCP-3 in CCR2-mediated recruitment of inflammatory monocytes during Listeria monocytogenes infection. 2008; 180:6846–6853.
41. Bae WK, Umeyama A, Chung IJ, Lee JJ, Takei M. Uncarinic acid C plus IFN-gamma generates monocyte-derived dendritic cells and induces a potent Th1 polarization with capacity to migrate. 2010; 266:104–110.
42. Karlmark KR, Weiskirchen R, Zimmermann HW, Gassler N, Ginhoux F, Weber C, Merad M, Luedde T, Trautwein C, Tacke F. Hepatic recruitment of the inflammatory Gr1+ monocyte subset upon liver injury promotes hepatic fibrosis. 2009; 50:261–274.
43. Kusmartsev S, Cheng F, Yu B, Nefedova Y, Sotomayor E, Lush R, Gabrilovich D. All-trans-retinoic acid eliminates immature myeloid cells from tumor-bearing mice and improves the effect of vaccination. 2003; 63:4441–4449.

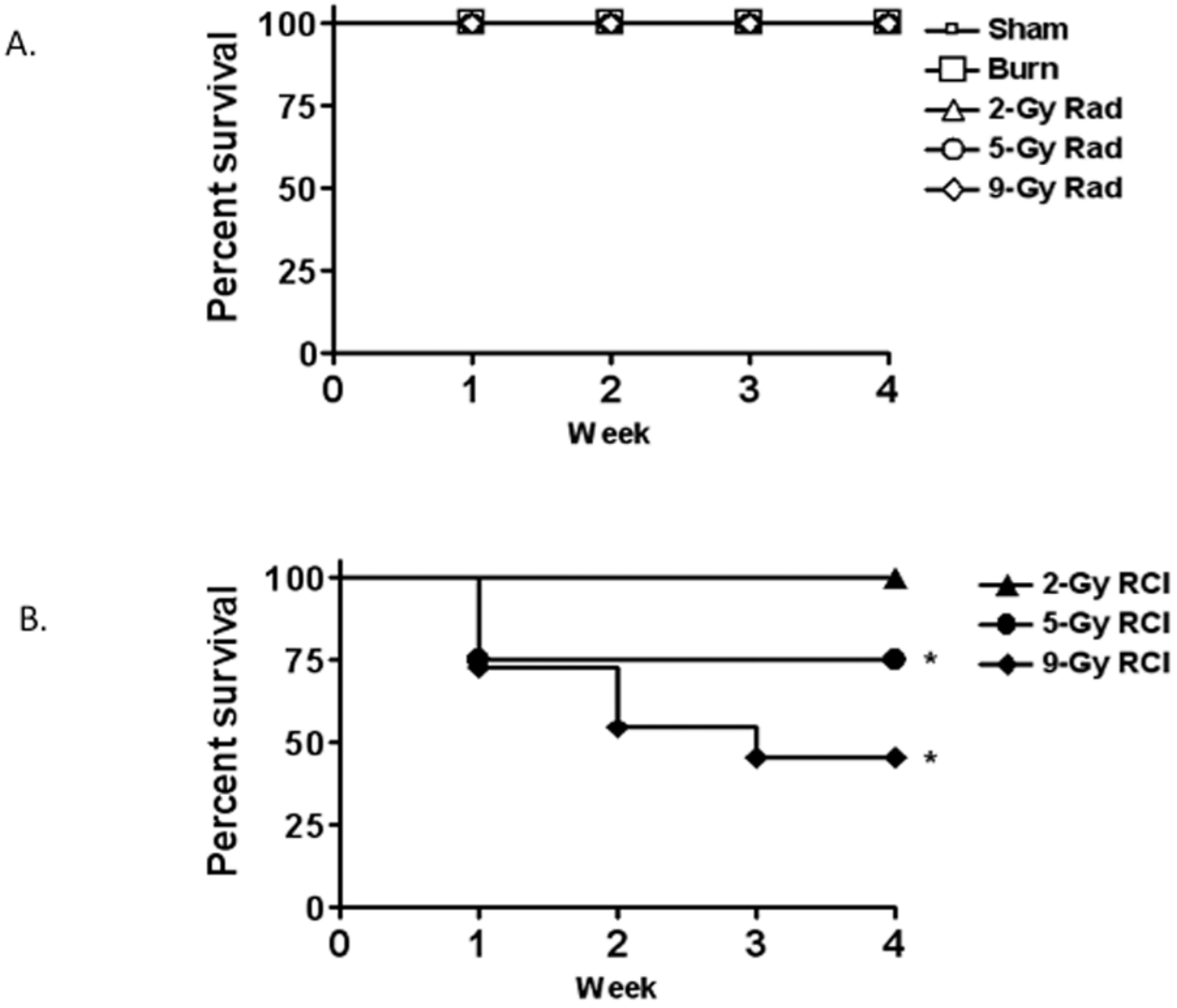

Figure 1. Survival is decreased after RCI when radiation doses exceed 5-Gy

A) C57BL/6 mice received either sham injury, burn injury (20% TBSA, full-thickness burn), or radiation exposure (2-, 5-, 9-Gy). B) C57BL/6 mice received a thermal injury (20%TBSA, full-thickness burn) followed by radiation exposure (2-, 5- 9-Gy). Survival was observed up to 4 weeks. Data is expressed as percent survival. Groups include 9–12 mice; *P<0.05 vs. sham group.

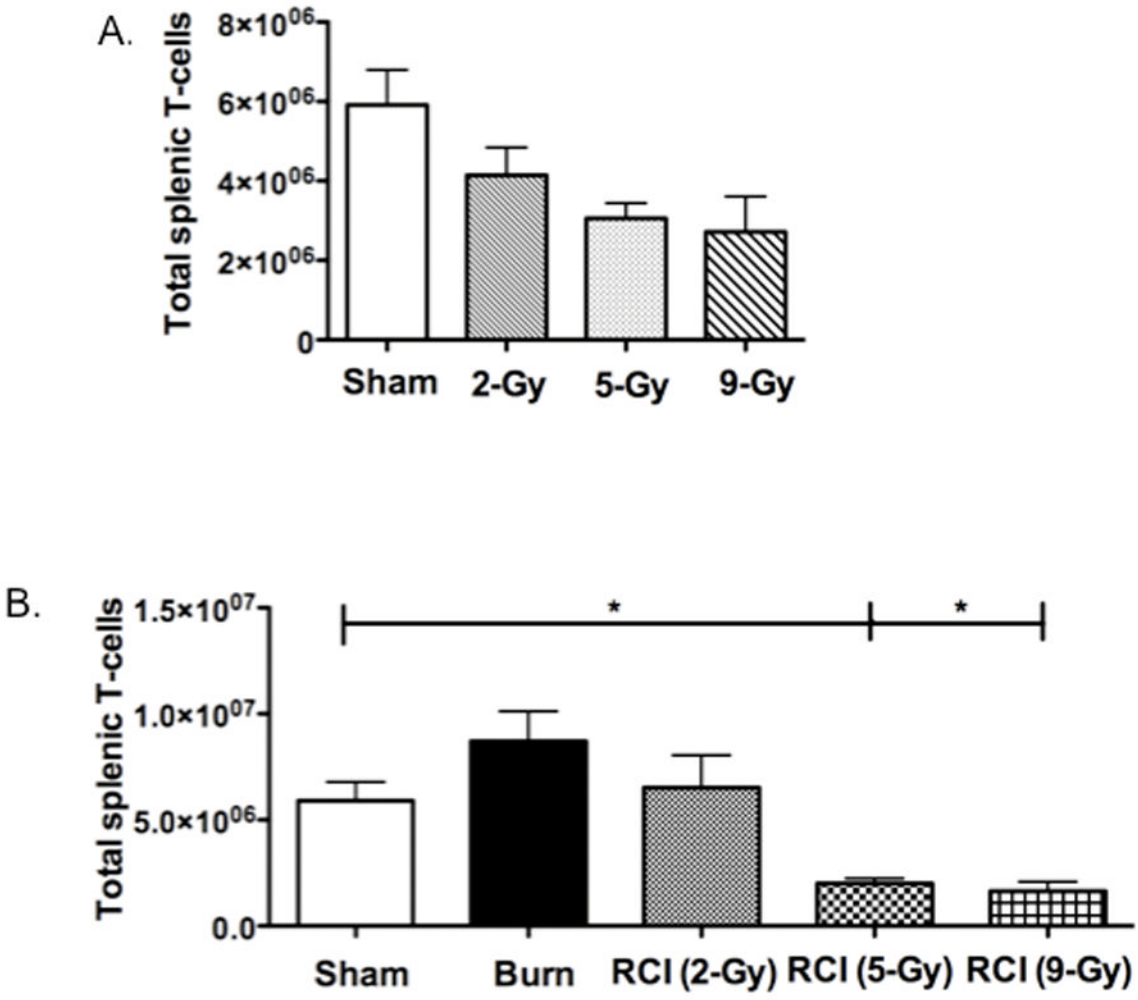

Figure 2. Lymphopenia is radiation dose-dependent

A) C57BL/6 mice received either sham injury or radiation exposure (2-, 5-, 9-Gy). Spleens were harvested at day 21 post-injury. Flow cytometry was performed to quantify the total number of splenic $CD4^+$ and $CD8^+$ T-cells. B) C57BL/6 mice received either sham, burn (20%TBSA, full-thickness burn), or thermal injury (20%TBSA, full-thickness burn) followed by radiation exposure (2-, 5- 9-Gy). Spleens were harvested at day 21 post-injury. Flow cytometry was performed to quantify the total number of splenic $CD4^+$ and $CD8^+$ T-cells. Groups include 10–12 mice; *$P<0.05$.

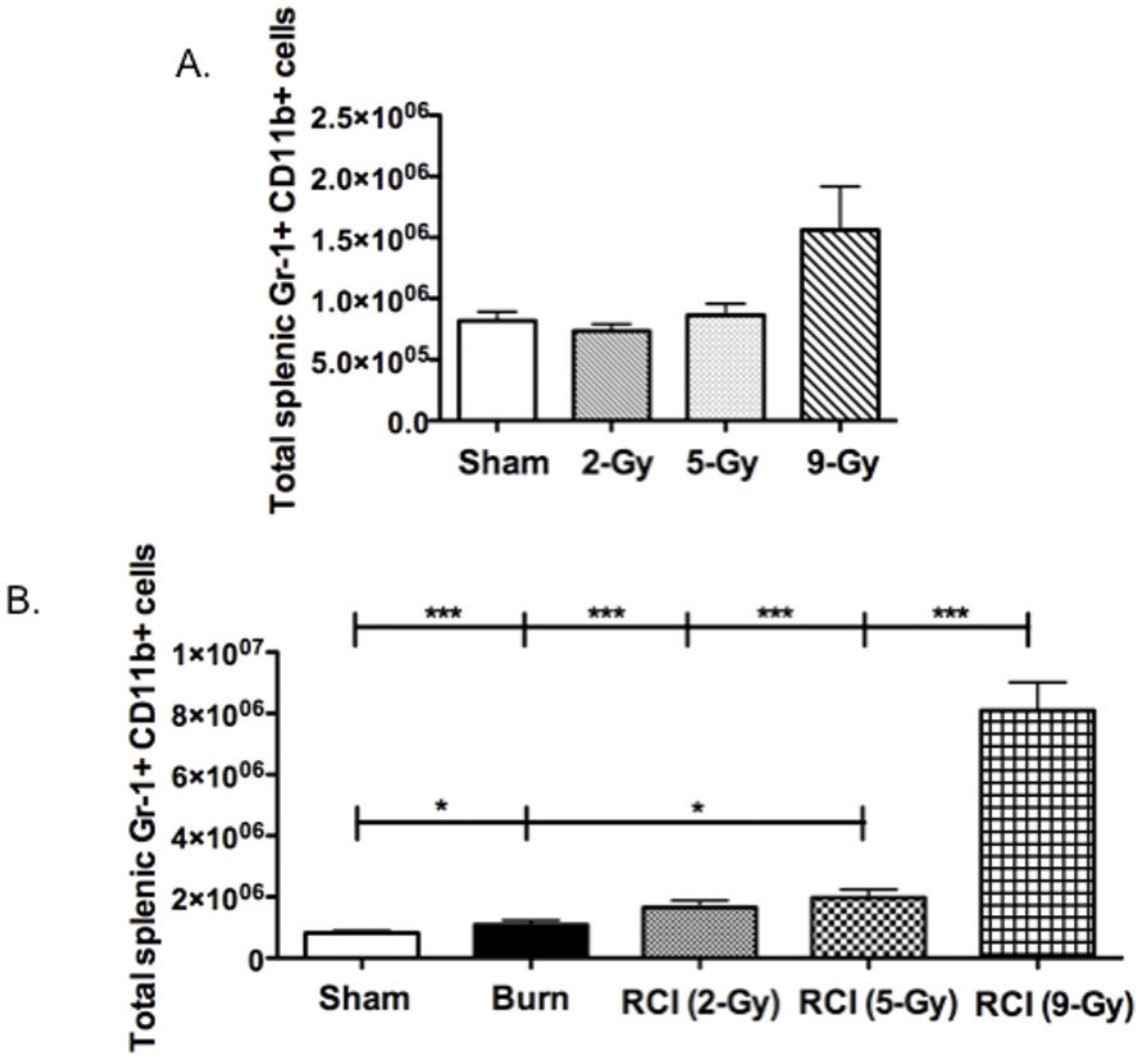

Figure 3. Gr-1^{+}CD11b^{+} cells are elevated after RCI at day 21

A) C57BL/6 mice received either sham injury or radiation exposure (2-, 5-, 9-Gy). Spleens were harvested at day 21 post-injury. Flow cytometry was performed to quantify the total number of splenic Gr-1^{+}CD11b^{+} cells. B) C57BL/6 mice received either sham, burn (20%TBSA, full-thickness burn), or thermal injury (20%TBSA, full-thickness burn) followed by radiation exposure (2-, 5- 9-Gy). Spleens were harvested at day 21 post-injury. Flow cytometry was performed to quantify the total number of splenic Gr-1^{+}CD11b^{+} cells. Groups include 10–12 mice; *P<0.05.

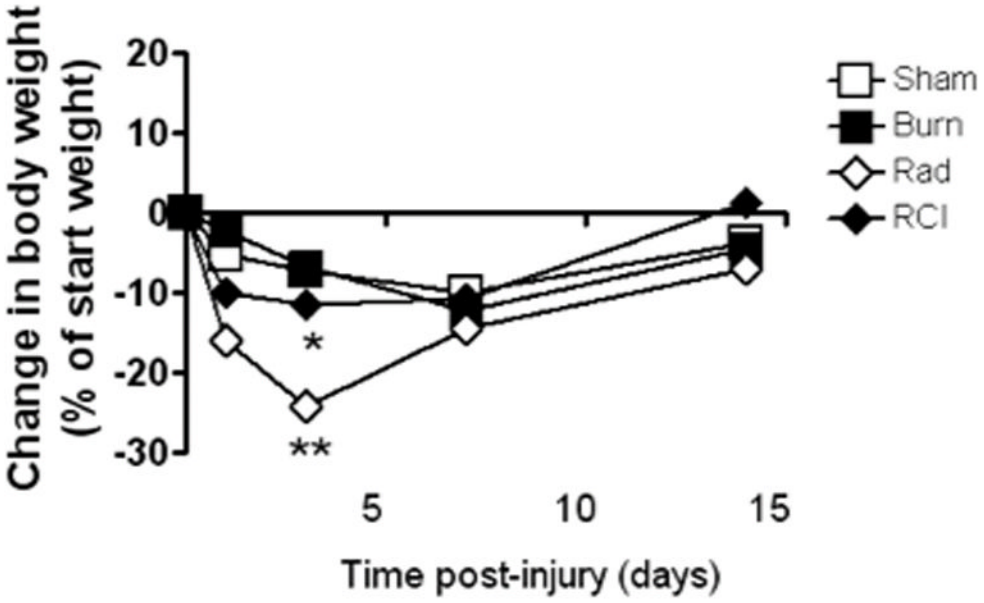

Figure 4. Significant weight loss is observed by three days post-radiation exposure (5-Gy) and RCI (20%TBSA+5-Gy)

C57BL/6 mice received either sham injury, burn injury (20% TBSA, full-thickness burn), radiation exposure (5-Gy) or RCI (20% TBSA + 5-Gy). Body weight (g) of mice was measured at days 0, 3, 7 and 14 post-injury. Experiments were repeated in triplicate. Groups include 3–7 mice. *P<0.05, **P<0.01 vs. sham group.

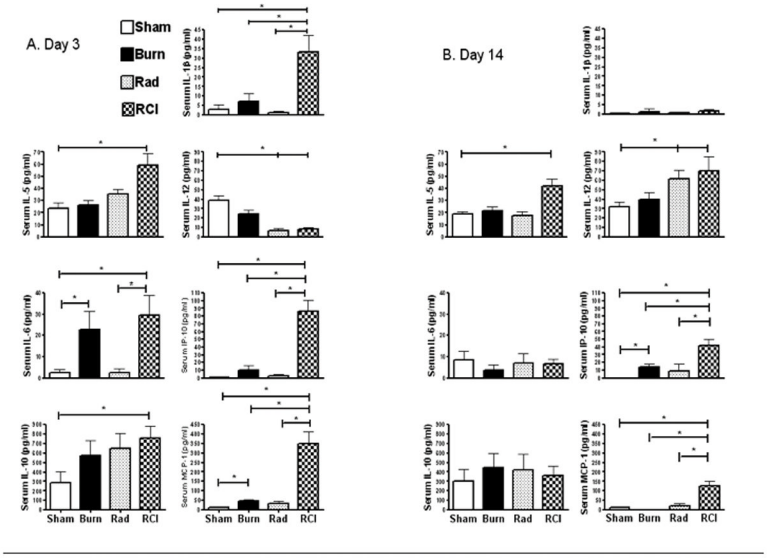

Figure 5. RCI (20%TBSA+5-Gy) increases pro-inflammatory serum cytokines at day 3 and 14

C57BL/6 mice received either sham injury, burn injury (20% TBSA, full-thickness burn), radiation exposure (5-Gy) or RCI (20% TBSA + 5-Gy). Serum was collected by cardiac puncture on the day of harvest. Serum cytokines of sham, burn, radiation and RCI mice at day 3 (A) and day 14 (B) were analyzed by multiplex bead array. Each experimental time point was repeated. Groups consist of 4–6 mice; *P<0.05.

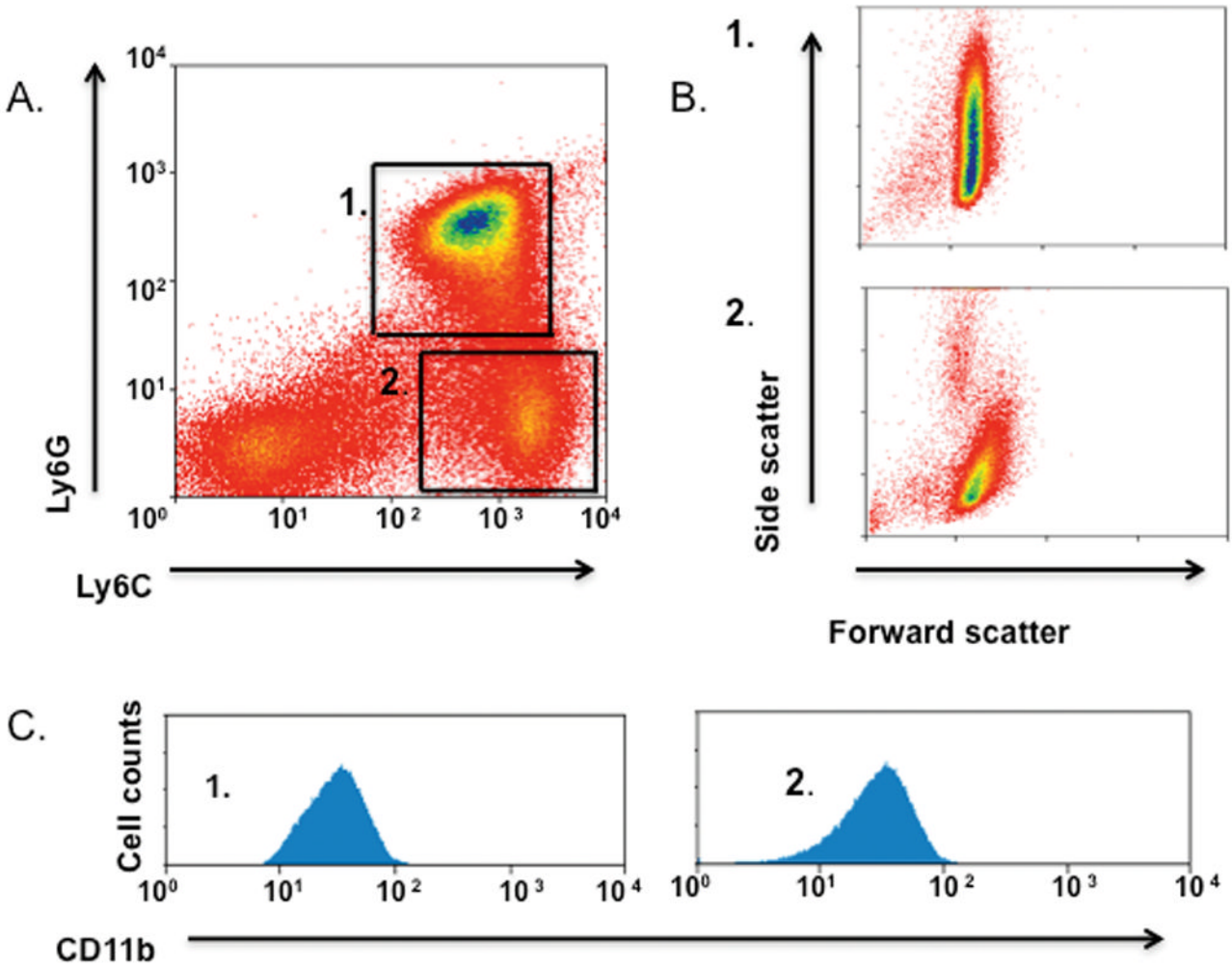

Figure 6. Gr-1^{+}CD11b^{+} cells consist of a heterogenous population of Ly6G^{+}Ly6C^{+} and Ly6C^{+}Ly6G^{-} myeloid cells

Gr-1^{+}CD11b^{+} cells were further defined by their Ly6C and Ly6G expression. A) A heterogenous population of CD11b^{+} cells were identified and consisted of Ly6G^{+}Ly6C^{+} and Ly6C^{+}Ly6G^{-} cells. B) Side scatter and forward scatter of light suggest that 1.) the Ly6G^{+}Ly6C^{+} population is granulocytic with high side scatter consistent with increased granularity, and 2.) the Ly6C^{+}Ly6G^{-} population have intermediate side scatter consistent with a monocytic population. C) Histograms represent the CD11b expression of the gated cell populations.

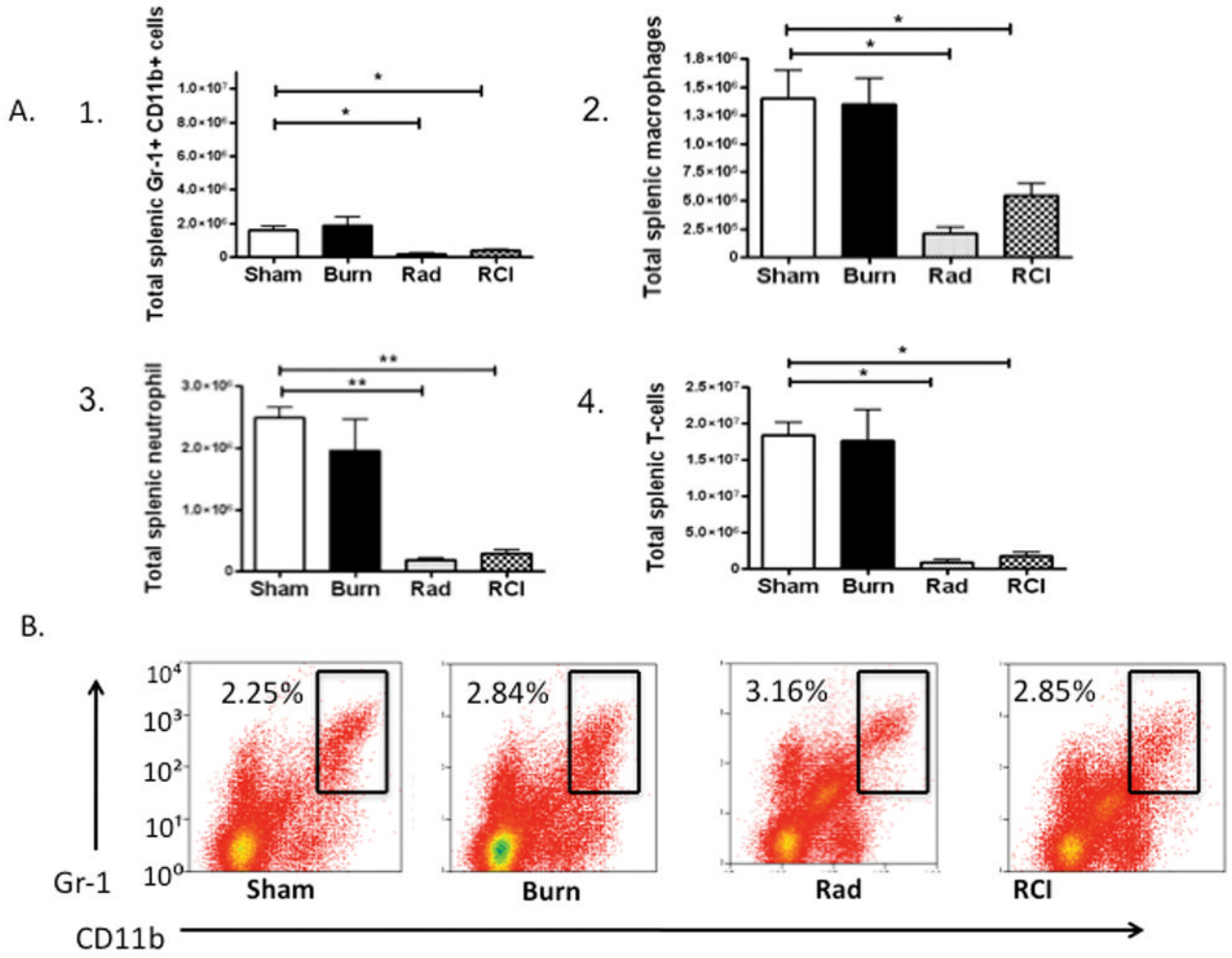

Figure 7. Innate and adaptive cell populations are reduced at day 3 after radiation (5-Gy) and RCI (20%TBSA+5Gy)

C57BL/6 mice received either sham injury, burn injury (20% TBSA, full-thickness burn), radiation exposure (5-Gy) or RCI (20% TBSA + 5-Gy). Spleens were harvested from sham, burn, radiation, and RCI mice at day 3. A) Cell populations were identified by cell surface markers using flow cytometric staining. B) Rectangle gates represent the proportion of $Gr\text{-}1^{+}$ $CD11b^{+}$ cells within each histogram. Experiments were repeated. Each group consists of 4–5 mice; *P<0.05, **P<0.001 vs. sham group.

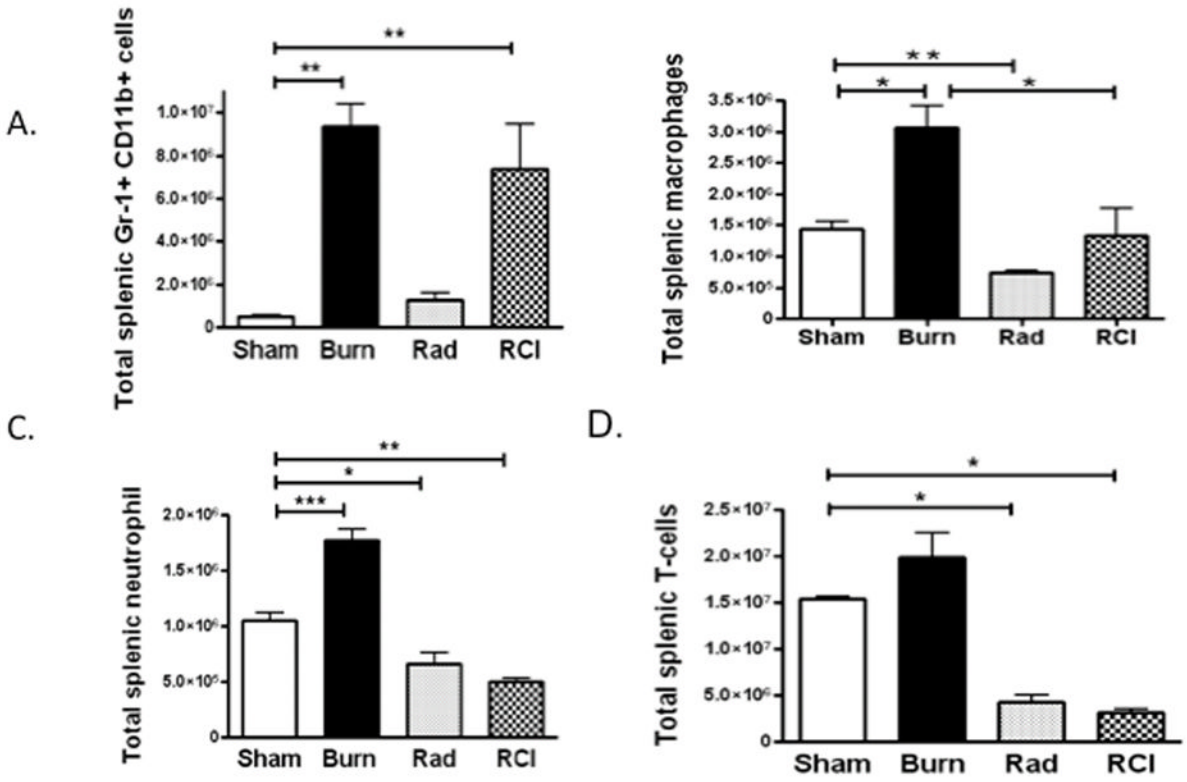

Figure 8. Gr-1$^+$ CD11b$^+$ cells are elevated at day 14 after burn (20%TBSA) and RCI (20%TBSA+5-Gy)

C57BL/6 mice received either sham injury, burn injury (20% TBSA, full-thickness burn), radiation exposure (5-Gy) or RCI (20% TBSA + 5-Gy). Spleens were harvested from sham, burn, radiation (5-Gy) and RCI (20%TBSA+5-Gy) at day 14. Cell populations were identified by cell surface markers using flow cytometric staining. Experiments were repeated four times. Each group consists of 4–7 mice. *P<0.05, **P<0.01 ***P<0.001.

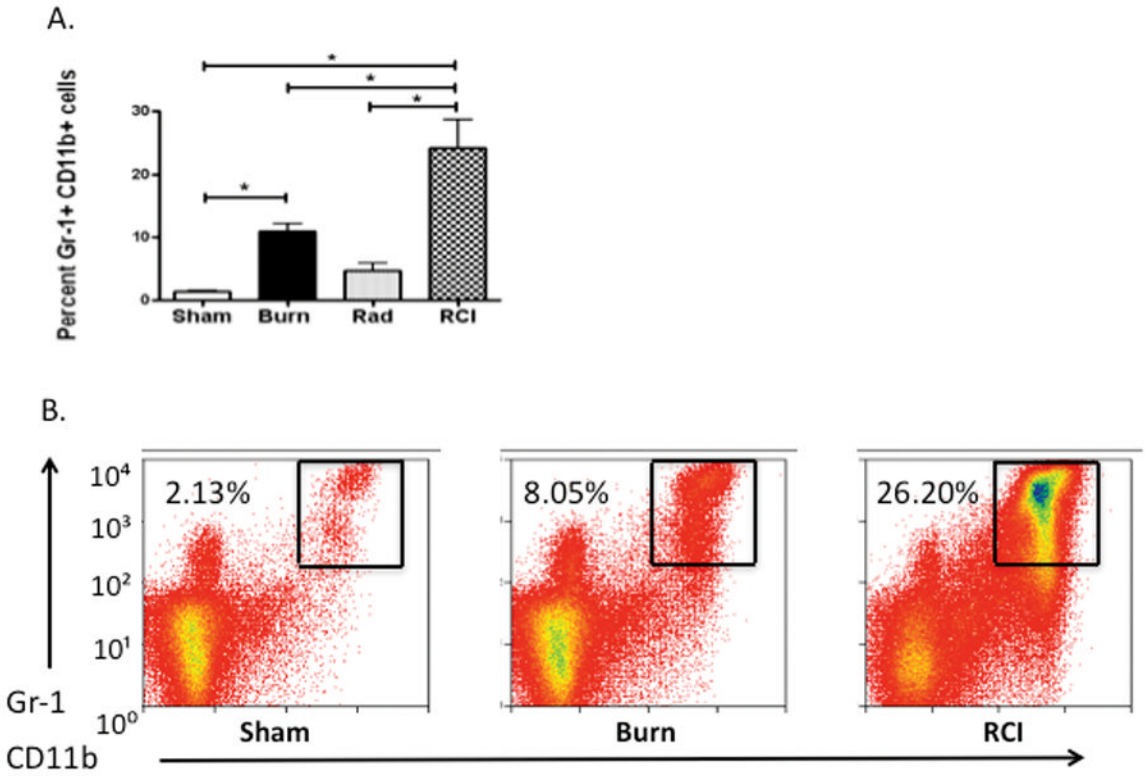

Figure 9. Gr-1$^+$CD11b$^+$ cells are a major cell type at day 14 after RCI (20%TBSA+5-Gy)

C57BL/6 mice received either sham injury, burn injury (20% TBSA, full-thickness burn), radiation exposure (5-Gy) or RCI (20% TBSA + 5-Gy). Spleens were harvested from sham, burn, radiation (5-Gy) and RCI (20%TBSA+5-Gy) at day 14. A) Percent of splenic Gr-1$^+$ CD11b$^+$ cells in each experimental group were determined by flow cytometry. B) Rectangle gates represent percent of Gr-1$^+$CD11b$^+$ cells within each histogram. Experiments were repeated four times. Each group consists of 4–7 mice. *P<0.05, **P<0.01 ***P<0.001.

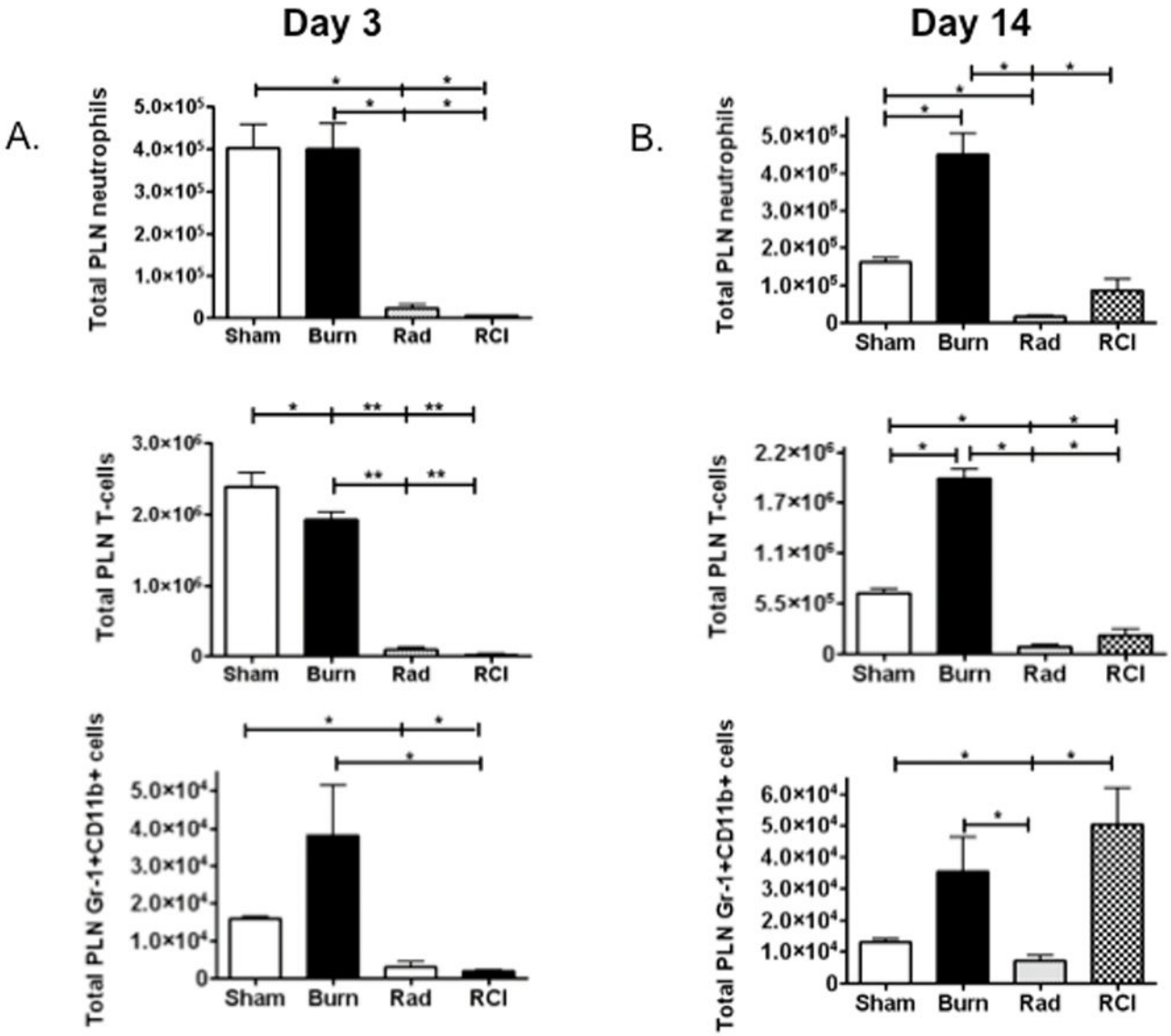

Figure 10. Gr-1$^+$CD11b$^+$ cells are increased in the PLN after RCI

C57BL/6 mice received either sham injury, burn injury (20% TBSA, full-thickness burn), radiation (5-Gy) or RCI (20%TBSA + 5-Gy). A) At day 3 and B) day 14 inguinal and axillary lymph nodes (PLN) were harvested and pooled together. Cell populations were identified by cell surface markers using flow cytometric staining. Experiments were repeated. Each group consists of 4–7 mice. *P<0.05.

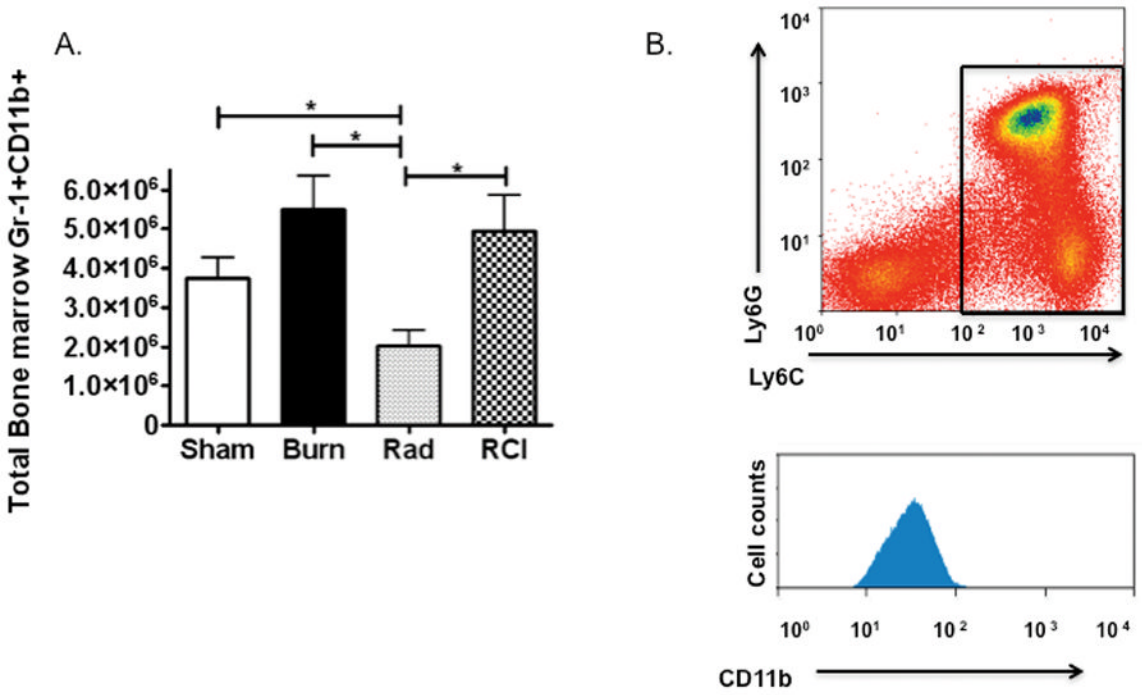

Figure 11. A heterogeneous population of Gr-1$^+$CD11b$^+$ myeloid cells is observed in the bone marrow at day 14

C57BL/6 mice received either sham injury, burn injury (20% TBSA, full-thickness burn), radiation (5-Gy) or RCI (20%TBSA + 5-Gy). Bone marrow was harvested from bilateral femurs at day 14. A) Populations of Gr-1$^+$CD11b$^+$ cells were identified by cell surface markers using flow cytometric staining. B) Gr-1$^+$CD11b$^+$ cells in the bone marrow consist of a heterogeneous Ly6G$^+$Ly6C$^+$ and Ly6C$^+$Ly6G$^-$ populations.

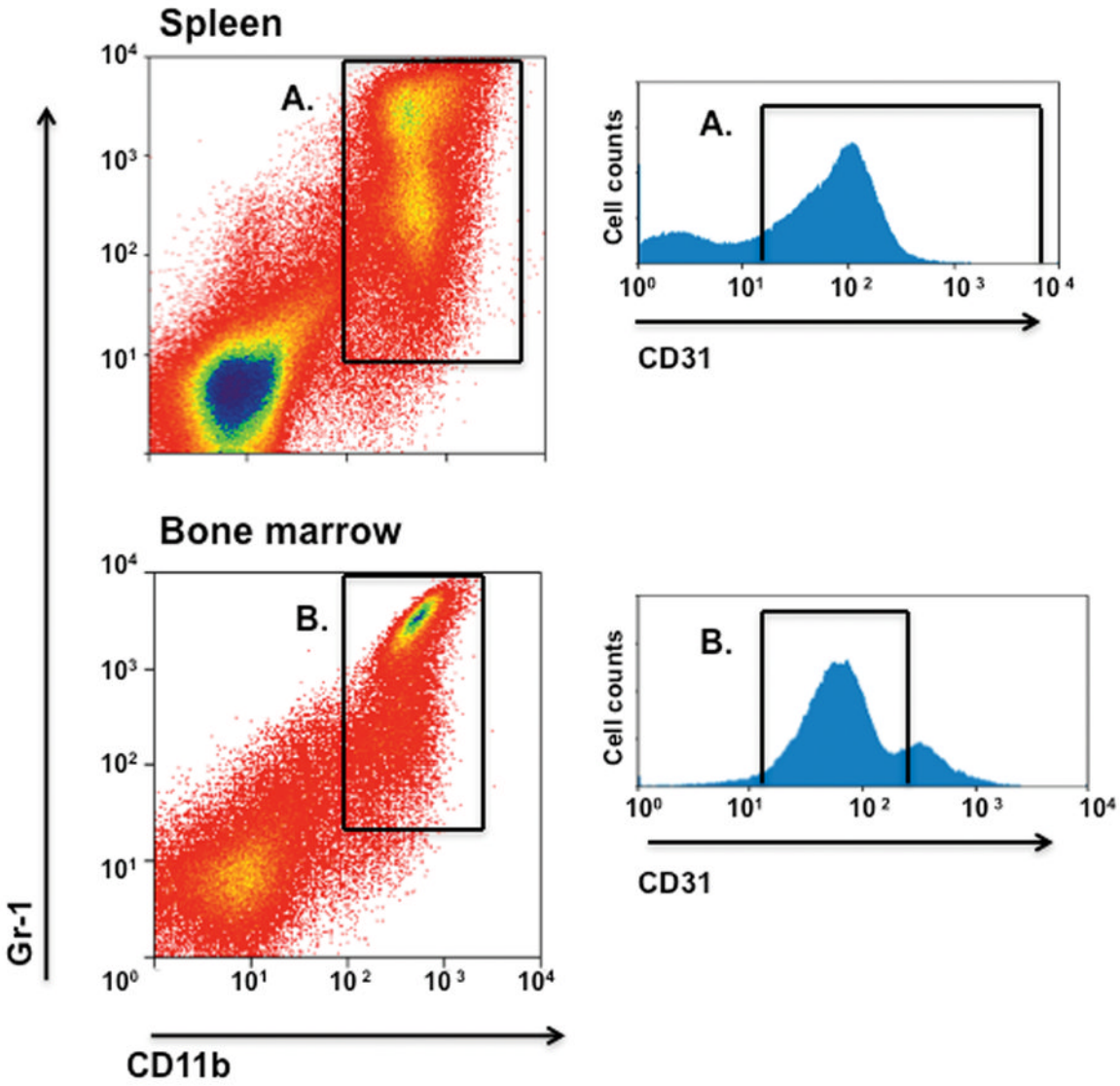

Figure 12. Gr-1^{+}CD11b^{+} cells after RCI express cell surface markers consistent with immature and blast myeloid progenitors

A) Spleens and B) bone marrow were harvested at day 14 from RCI (20%TBSA + 5-Gy) mice. Gr-1^{+}CD11b^{+} cells were identified by cell surface markers using flow cytometric staining. Rectangle gates represent Gr-1^{+}CD11b^{+} cells and their CD31 (PECAM) expression.

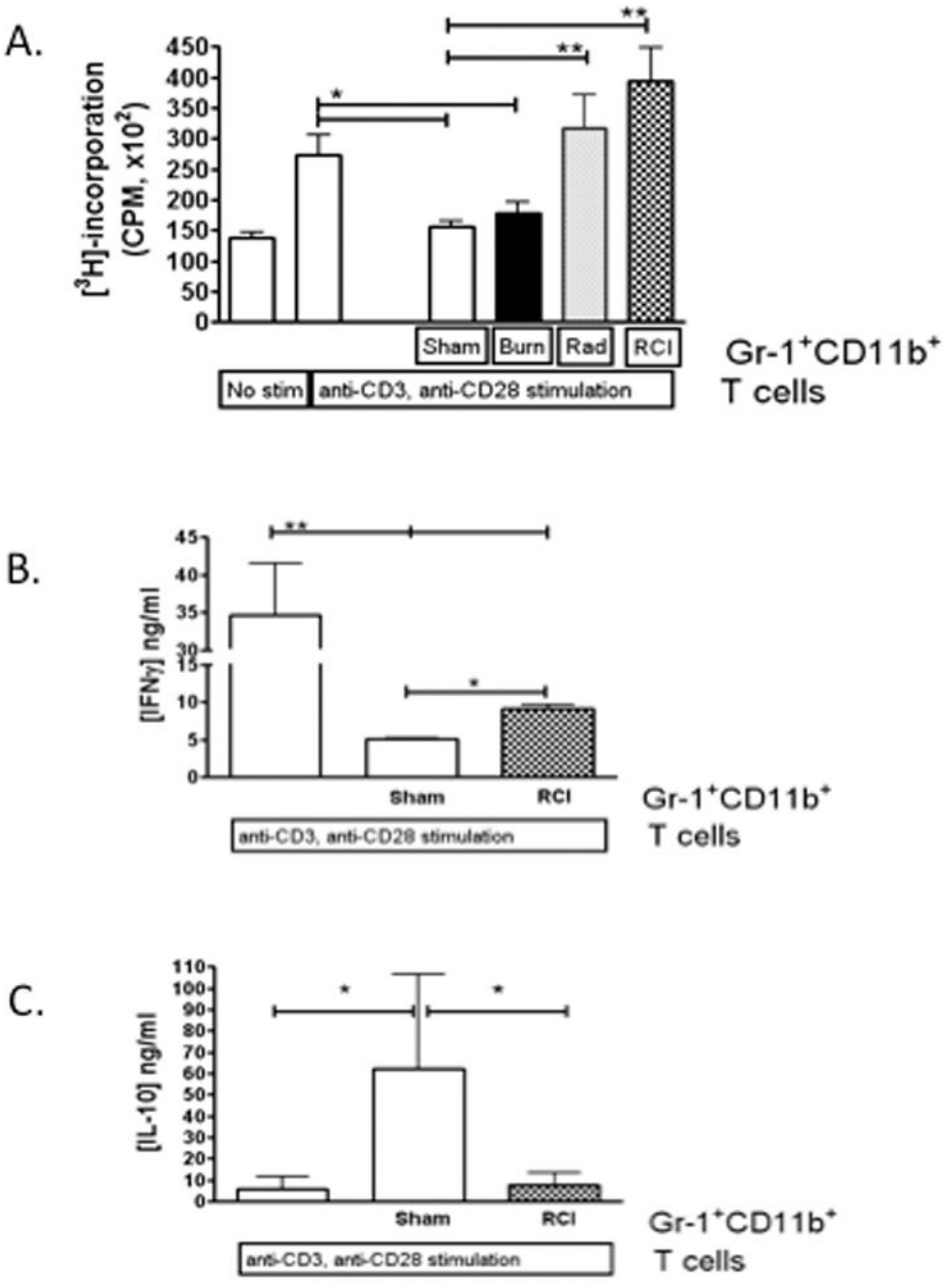

Figure 13. Thymidine incorporation by T-cells is increased after co-culture with Gr-1$^+$ CD11b$^+$ cells from radiation (5-Gy) and RCI (20%TBSA+5-Gy) mice

C57BL/6 mice received either sham injury, burn injury (20% TBSA, full-thickness burn), radiation exposure (5-Gy) or RCI (20% TBSA + 5-Gy). Spleens were harvested from sham, burn, radiation (5-Gy) and RCI (20%TBSA+5-Gy) at day 14. Cells were harvested from spleens. Gr-1$^+$CD11b$^+$ cells were sorted and purified by FACS from single cell suspensions. T-cells were purified from untouched C57BL/6 spleens by negative magnetic selection. T-cells were then cultured with plate bound anti-CD3, soluble anti-CD28 and Gr-1$^+$ CD11b$^+$ cells (ratio 1:1; T-cell: Gr-1$^+$ CD11b$^+$ cells) for 72 hours. Controls included stimulated and unstimulated T-cells. [^{3}H]-thymidine was pulsed during the last 18 hours of culture. Proliferation is expressed as cpm [^{3}H]-thymidine incorporation. Experiments were repeated

in triplicate. Groups consist of 6–7 mice; *P<0.05, **P<0.01. B, C). Supernatants were collected prior to the addition of [^{3}H]-thymidine, and analyzed by multiplex bead array. IFN-γ (B) and IL-10 (C) were analyzed and compared between RCI, sham and stimulated T-cell controls (±SEM; n=6–7); *P<0.05, **P<0.01.

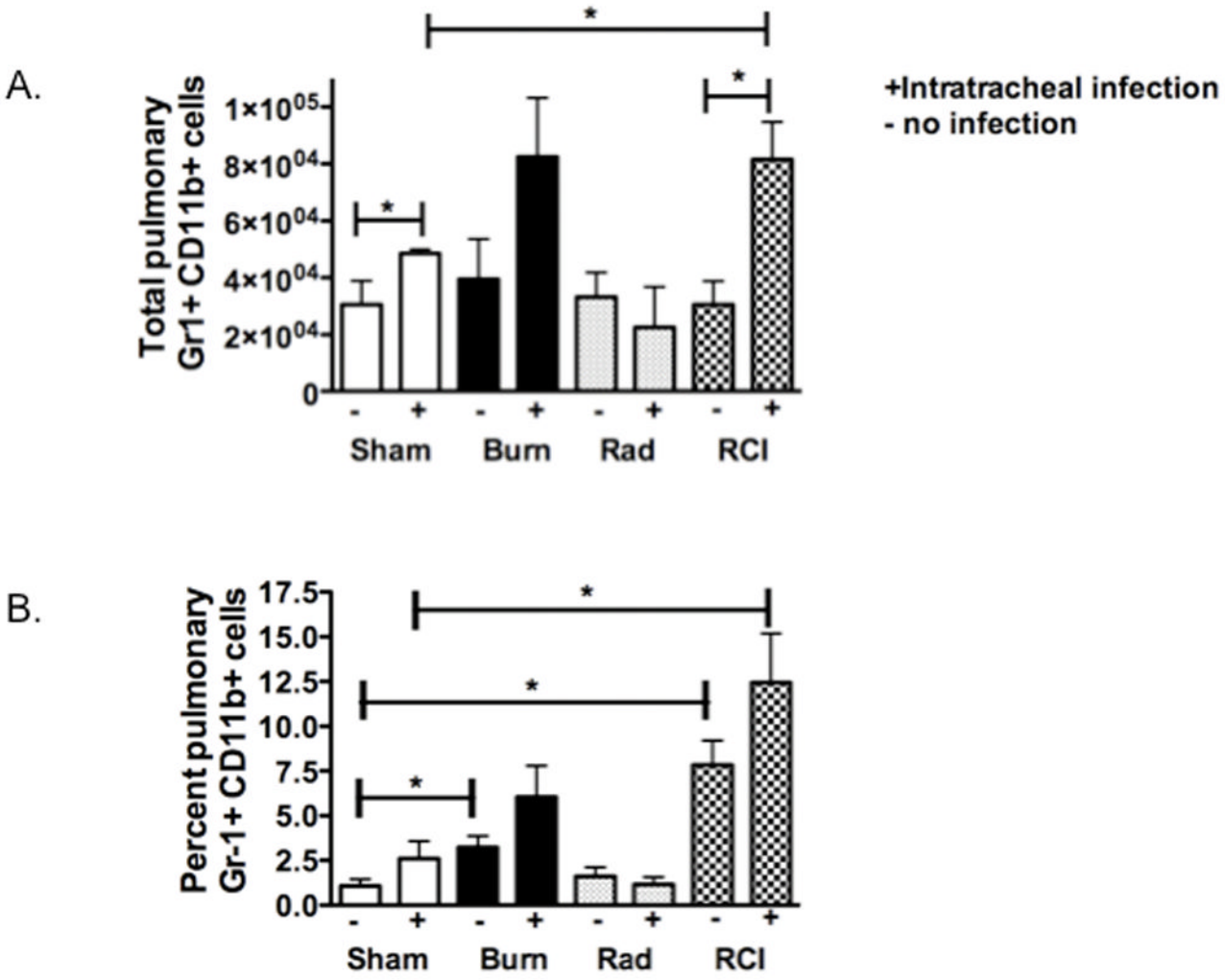

Figure 14. Gr-1$^+$CD11b$^+$ cells recruit to the lung after pulmonary infection

C57BL/6 mice sustained either sham injury, burn injury (20% TBSA, full-thickness burn), radiation exposure (5-Gy) or RCI (20% TBSA + 5-Gy). Each experimental group was infected at day 14 post-injury with (1×10^7cfu/inoculum) by intratracheal inoculation; another group remained uninfected. Lung was harvested 24 hours after infection. One lobe was further processed into a single cell suspension. Gr-1$^+$CD11b$^+$ cells were identified by cell surface markers using flow cytometric staining. A) Total Gr-1$^+$CD11b$^+$ cell numbers were enumerated and analyzed. B) Percent of Gr-1$^+$CD11b$^+$ cells in each experimental group were quantified by flow cytometry (±SEM; n=4–5); *P<0.05.

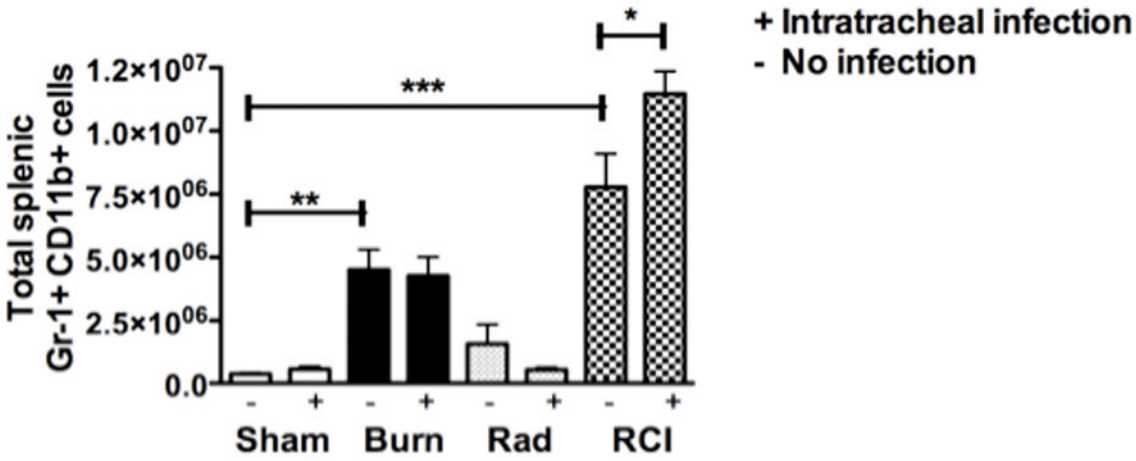

Figure 15. Splenic Gr-1$^+$CD11b$^+$ cells in RCI mice increase after pulmonary infection

C57BL/6 mice received either sham injury, burn injury (20% TBSA, full-thickness burn)radiation exposure (5-Gy) or RCI (20% TBSA + 5-Gy). Each experimental group was infected at day 14 post-injury with (1×10^7cfu/inoculum) by intratracheal inoculation.; another group remained uninfected. Spleens were harvested 24 hours after infection. Gr-1$^+$CD11b$^+$ cells were identified by cell surface markers using flow cytometric staining. Total Gr-1$^+$CD11b$^+$ cell numbers were enumerated and analyzed (±SEM; n=4–5); *P<0.05.

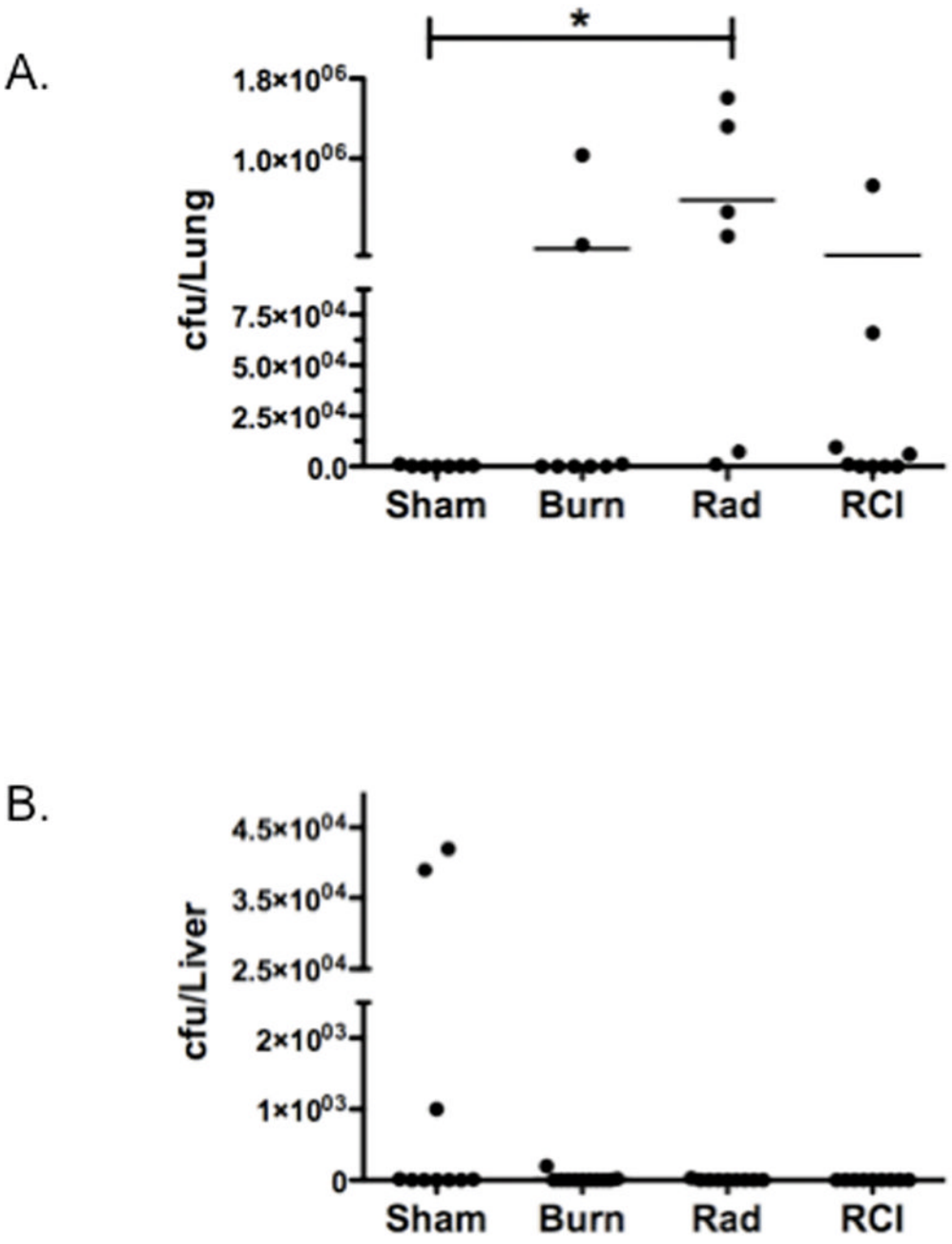

Figure 16. Pulmonary microbial clearance is similar among sham, burn and RCI mice, but decreased in radiation (5-Gy) mice

C57BL/6 mice received either sham injury, burn injury (20% TBSA, full-thickness burn), radiation exposure (5-Gy) or RCI (20%TBSA + 5-Gy). Each experimental group was infected at day 14 post-injury with (1×10^7cfu/inoculum) by intratracheal inoculation. A) Lung was harvested 24 hours after infection. One lobe was homogenized and inoculated onto tryptic soy agar containing kanamycin (25mg/mL) (TSA-k). Colony-forming units were enumerated per plate at 24 hours post-harvest (±SEM; n=6–9); *P<0.05. B) Liver was harvested 24 hours after infection. The entire organ was homogenized and inoculated onto TSA-k. Colony-forming units were enumerated per plate at 24 hours post-harvest (±SEM; n=10–11).